
ELSEVIER

Journal of Non-Crystalline Solids 303 (2002) 101–107

JOURNAL OF
NON-CRYSTALLINE SOLIDS

www.elsevier.com/locate/jnoncrysol

Modelling of point defects in monoclinic zirconia

A.S. Foster [a,*], V.B. Sulimov [b], F. Lopez Gejo [b], A.L. Shluger [b], R.M. Nieminen [a]

[a] *Laboratory of Physics, Helsinki University of Technology, P.O. Box 1100, 02015 Helsinki, Finland*
[b] *Department of Physics and Astronomy, University College London, Gower Street, London WC1E 6BT, UK*

Abstract

We present the results of plane wave density functional theory calculations of oxygen vacancies and interstitial oxygen atoms in monoclinic zirconia. After calculating the incorporation energies and structures of interstitial oxygen atoms and formation energies of neutral oxygen vacancies, we consider the electron affinities and ionisation potentials of these defects. These properties are especially important at the silicon/oxide interface in MOSFET devices, where silicon may serve as an electron and hole source. The results demonstrate that interstitial oxygen atoms and positively charged oxygen vacancies can trap electrons if the electron source (band offset) is higher than ~2 eV above the top of the zirconia valence band.

PACS: 77.22.C

1. Introduction

Recently zirconia related research has received a boost due to an intensive search for new dielectric materials capable of substituting silicon dioxide in its role as gate dielectric in many microelectronic devices. Thin ZrO_2 films grown on silicon demonstrate favourable parameters, such as high thermal stability and low leakage current [1,2]. High resolution TEM indicated the presence of both tetragonal and monoclinic phases in these films [2], and therefore studies of defect properties in these zirconia phases have become extremely topical. In this paper we present the results of the plane wave density functional theory (DFT) calculations of oxygen vacancies and interstitial oxygen atoms in monoclinic zirconia. An expanded paper on this work with greater detail and discussion can be found in [3].

2. Method

All the calculations have been performed using the plane wave basis VASP code [4,5], implementing spin-polarized DFT and the generalized gradient approximation (GGA). We have used ultrasoft Vanderbilt pseudopotentials [6,7] to represent the core electrons. In order to validate both the pseudopotentials and the method itself, extensive calculations were performed on the three dominant bulk phases of zirconia: cubic, tetragonal and monoclinic. In all cases the agreement between calculated and experimental values

* Corresponding author. Tel.: +358-9 451 3103; fax: +358-9 451 3116.
E-mail address: asf@fyslab.hut.fi (A.S. Foster).

0022-3093/02/$ - see front matter
PII: S0022-3093(02)00974-2

was excellent [3], demonstrating that both the pseudopotentials and method are suitable for this study.

All defect calculations were made with a 96 (±1) atom unit cell, which is generated by extending the 12 atom monoclinic unit cell by two in all three dimensions. For this cell, the total energy was found to converge to 10 meV for a plane cutoff of 500 eV and 2 k-points. The large size of the cell separates the periodic defect images by over 10 Å, greatly reducing the unphysical interactions between them. For geometry relaxation we used a combination of conjugate-gradient energy minimization and quasi-Newton force minimization. During defect calculations the lattice vectors of the cell were frozen and all atoms were allowed to relax until atomic forces were less than 0.05 eV/Å.

A neutralizing background was applied to the unit cell for calculations of charged defects. The fact that the zero one-electron energy level remained in a consistent position with respect to the zirconia valence band in all defect calculations gives us confidence that this method gives a good representation of an isolated defect in an infinite non-defective crystal.

The vacancy formation energies $E_{\text{for}}(\text{defect})$ (or equivalently, the oxygen incorporation energies) were calculated for the fully relaxed geometry of the defected supercell ($E(\text{defect})$) with respect to the perfect monoclinic 96 atom unit cell ($E(\text{per})$) and an isolated oxygen atom ($E(\text{O})$) according to

$$E_{\text{for}}(\text{defect}) = E(\text{defect}) - (E(\text{per}) + E(\text{O})). \qquad (1)$$

3. Point defects

3.1. Oxygen interstitials

Four possible interstitial defects (O^0, O^-, O^{2-}, O^+) have been considered in this study. Further, each interstitial can form a stable defect pair with either a tetragonally (tetra) or triply bonded (triple) lattice oxygen (see Fig. 1), hence a total of seven interstitial defect systems are investigated (the hole on oxygen has only been considered for the X_3 site). For ease of reference all values associated with a triply bonded oxygen will be labelled X_3 and all associated with a tetragonally bonded oxygen will be labelled X_4, where X is the defect species.

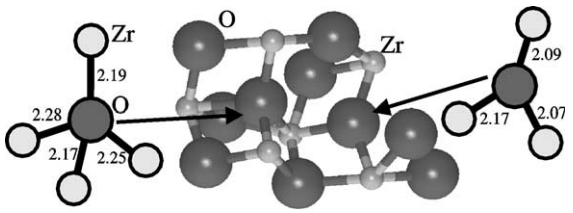

Fig. 1. Diagram showing the tetragonal (left) and triple-planar (right) bonding of the oxygen ions in the monoclinic phase of zirconia as calculated in this work. Distances are in Å.

The atomic oxygen formation energy relative to the non-defective zirconia structure and half of the energy of an isolated O_2 molecule, $E(\text{O})$, (see Eq. (1)) is +1.4 eV for O_3^0 and +2.2 eV for O_4^0. A positive value indicates an endothermic process, which involves dissociation of the O_2 molecule. Subtracting half of the theoretical dissociation energy, which is equal 5.88 eV in our calculations, from $E(\text{O})$ gives the energy of an oxygen atom in a triplet state as −1.97 eV, and we find that a single O atom is incorporated in the monoclinic zirconia lattice with an energy gain of −1.6 eV (O_3^0) and −0.8 eV (O_4^0). These values are close to those found for the oxygen formation in zircon ($ZrSiO_4$) [8]. They can be also compared with those reported in the literature for the same process in alpha-quartz. Using a periodic LDA approach Hamann has found an formation energy of −0.86 eV [9]; a similar value, −0.7 eV has been reported from correlated cluster calculations [10], and −0.9 eV in recent DFT GGA-II calculations [11].

Below we discuss the electron-trapping properties of interstitial oxygen sites. For the O_4^0 site, we found that when extra electrons are added to the system, there is no stable energy minimum for the oxygen interstitial near to the tetragonal site. In fact the interstitial undergoes large displacements and moves to the most easily available triple oxygen site, forming an O_3^- defect. Due to this and since the triple oxygen site (O_3^0) in zirconia is energetically favoured for interstitial formation, we will now focus in detail only on defects incorporated at that site.

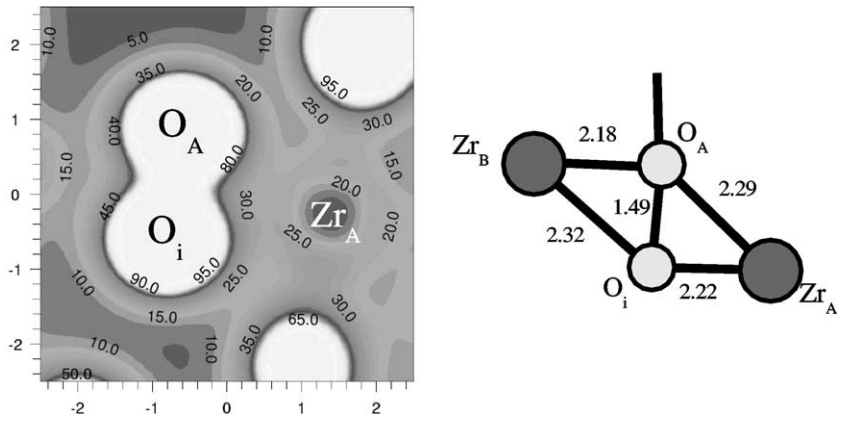

Fig. 2. Charge density and schematic diagram of neutral oxygen interstitial (O_i) near a triply bonded oxygen (O_A) in zirconia. Charge density is in 0.1 e/Å and all distances are in Å.

Fig. 2 shows the fully relaxed charge density and position of ions near to a neutral oxygen interstitial. The charge density shows that the interstitial and lattice oxygen form a strong covalent bond, and effectively become a 'dumbbell' defect pair within the lattice. This configuration is similar to previous calculations of neutral oxygen interstitials in zircon [8], but differs from the 'peroxy-bridge' seen in silica calculations [11]. The lattice oxygen relaxes by up to 0.5 Å to accommodate the interstitial, distorting the original triple-planar O–Zr_3 group (see Fig. 1) into a slight pyramid with its apex pointing away from the interstitial. The Zr sublattice remains more or less undisturbed, with the nearest zirconium (Zr_A) to the pair only relaxing by around 0.05 Å. The defect is in the singlet state, with equal spin up and spin down components. Integration of the charge around the oxygens at a given radius gives the same values for both the interstitial and the lattice oxygen, indicating that significant charge has been transferred to the interstitial.

When one or two extra electrons were added to the system, they initially went to the conduction band and did not localise fully on the defect until after the system was relaxed. Effectively none of the oxygen interstitials have a significant vertical electron affinity. In fact the strong lattice relaxation is required to stabilise a charged defect. In particular, the introduction of the first extra electron to the neutral interstitial causes the interstitial and lattice oxygen to separate, both displacing by about 0.2 Å and also causing a 0.1 Å displacement of the Zr_A. Overall this reduces the covalent bond between them significantly. However, they remain effectively identical, with identical charge for a given radius. Calculation of the charge density difference between the system before and after the introduction of the electron show that the electron is completely localised on the defect pair.

For the final interstitial, the doubly charged oxygen interstitial in Fig. 3, the charge density and positions differ significantly to that demonstrated for the singly charged defect. The interstitial is now displaced significantly (about 0.5 Å) to accommodate the extra electron and occupies an effective new triple site (see Fig. 3), bonding with a third Zr ion. For the single charged interstitial, the third nearest Zr ion was over 2.5 Å from the interstitial and no bond could be seen in the charge density. In this new configuration, the oxygen ion forms slightly elongated bonds with the Zr ions compared to the normal lattice triple site. There is a corresponding reduction in the covalent bond between them. The defect remains in the singlet state, with equal spin components. Again, calculation of the charge density difference between the system before and after the introduction of the electron show that the electron is completely localised on O_i and O_A.

In order to study hole trapping, we have also simulated the case when an electron was removed

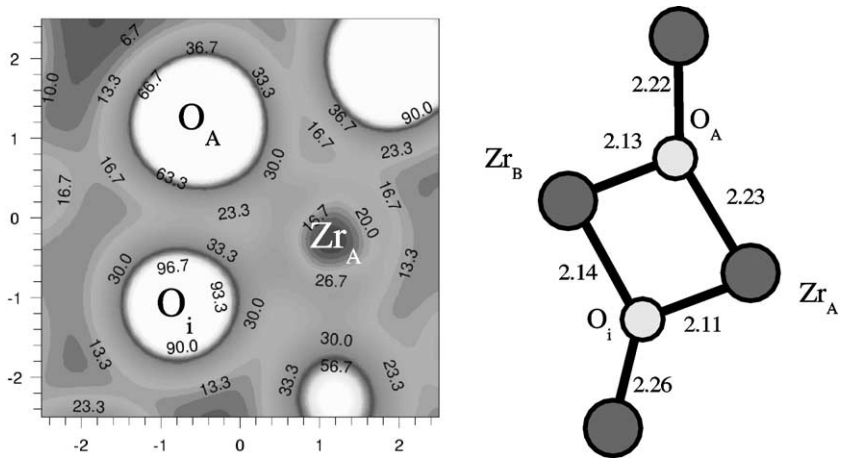

Fig. 3. Charge density and schematic diagram of doubly charged oxygen interstitial (O_i) near a triply bonded oxygen (O_A) in zirconia. Charge density is in 0.1 e/Å and all distances are in Å.

from the system with the neutral interstitial. However, the hole does not localise on the defect and remains almost completely delocalised. This may represent a well-known error in the kinetic energy calculated in DFT which favours delocalised over localised defect states and can also be seen for the V_4^- defect below. Therefore this result may not be accurate and will not be discussed in detail.

3.2. Vacancies

In respect of two types of oxygen atoms in monoclinic zirconia we considered vacancies of four and threefold coordinated oxygen: V_4 and V_3. The main properties of both types of vacancies are very similar and the discussion below is presented in terms of fourfold coordinated vacancy V_4, however, important differences between the two types will be emphasized.

We start our discussion from considering a neutral vacancy, which is formed by omitting one neutral oxygen atom from the 96 atom unit cell. Formation of the neutral vacancy leads to a very small relaxation of the four neighbouring Zr ions with displacements of only about 0.01–0.02 Å from their positions in the perfect crystal. The corresponding relaxation energy is ~0.11 eV. The vacancy formation energy is $E_{\text{for}}(V_4) = 8.90$ eV and $E_{\text{for}}(V_3) = 8.88$ eV. It is defined as $E_{\text{for}}(V) = E(\text{vacancy}) + E(O) - E(\text{perfect})$, where E(vacancy) and E(perfect) are the supercell energy for the defective and the perfect systems, respectively, and $E(O) = -1.97$ eV is the same as used for the interstitial calculations. We should note that the vacancy formation energy is quite similar to those obtained for silica and MgO (see, for example, [12,13]).

The neutral vacancy has a double-occupied energy level deep in the forbidden gap and is strongly localised. This energy level is situated ~2.2 eV above the top of the valence band. The maps of the corresponding charge density in the plane of three Zr neighbours shows that it is a bonding combination of atomic orbitals of all four Zr neighbours of the vacant site. Ionisation of the neutral oxygen vacancy results in the creation of the positively charged defect V_4^+. The remaining electron is strongly localised near the vacant site (it also reflects the bonding character of the charge density corresponding to the singly occupied localised state). The atomic relaxation in this case is much stronger than for the neutral vacancy: all four Zr neighbours move apart from the vacant site by about 0.1 Å and the relaxation energy amounts to 0.47 eV. Creation of the doubly positively charged vacancy V_4^{2+} is again accompanied by further displacement of the surrounding four Zr

ions which move apart from the vacant site by an additional 0.1 Å. This leads to an energy decrease of 0.74 eV. This behaviour of lattice relaxation is qualitatively similar to that for charged oxygen vacancies in MgO [13].

There have been suggestions that negatively charged vacancies (F′ centres [14]) can exist in zirconia. Therefore we also considered trapping of an additional electron at the neutral oxygen vacancy V_4^0 and creation of the negatively charged vacancy V_4^-. In this charged state the additional electron is only weakly localised in the vicinity of the vacancy. The corresponding spin maps clearly show strong delocalisation of the spin over the whole supercell. Therefore the atomic relaxation is very small: all four Zr neighbours displace by less than 0.02 Å and the energy decreases by less than 0.1 eV.

4. Defect levels

In order to study the possible role of defects in photo- and thermo-stimulated processes, and in electronic devices, one needs to know the position of defect states with respect to the bottom of the conduction band of zirconia or to other electron or hole sources, such as silicon. In this section we analyse the data obtained for the oxygen and vacancy defects from this perspective.

This analysis requires comparing energies of defects in different charge states. Several approaches to this analysis are possible, as discussed in Ref. [3]. In this work we apply a semi-empirical approach based on a common reference state Φ where electrons or holes originate. For example, in molecular calculations an electron after ionisation goes to infinity, where its energy is thought to be equal to zero. By analogy with a molecule, the difference in the total energy between the perfect lattice and that with one electron missing is the ionisation energy or the position of the top of the valence band with respect to the vacuum level. This energy in VASP calculations is negative and equal to about −1.78 eV. This means that the 'zero level' where the ionised electron goes in our calculations is at about −1.78 eV below the top of the valence band. This value is determined by the choice of pseudopotentials and the way the electrostatic Madelung potential is calculated. In real life, though, it should be somewhere above the bottom of the conduction band. Therefore, if electrons come to or go from the bottom of the conduction band, the energy of these electrons would be $\Phi = E_g(\text{exp}) + E(\text{per}, 0) - E(\text{per}, +)$ higher than the zero level in our calculations. Here $E_g(\text{exp})$ is the band gap. We should note that our calculated value of the band gap, 3.19 eV, is much smaller than any experimental or more accurate theoretical estimates available. In particular, the UPS data give 5.83 [15], EELS gives 4.2 eV [16], and the calculated GW corrected LDA value is 5.4 eV [17]. For the sake of simplicity, for further discussion we will use the UPS experimental value of $E_g(\text{exp}) = 5.83$ eV. This gives the reference energy as $\Phi = 5.83 + 1.78 = 7.61$ eV. Using this reference energy we can write further expressions for the the ionization potential, and electron and hole affinities as follows:

$$I_p(D) = E(D, q+1) + \Phi - E(D, q), \tag{2}$$

$$\chi_e(D) = E(D, q) - E(D, q-1) + \Phi, \tag{3}$$

$$\chi_h(D) = E(D, q) - E(D, q+1) - \Phi + E_g(\text{exp}). \tag{4}$$

We present the calculated values in Table 1 and the electron affinities are also shown in a schematic energy diagram in Fig. 4.

Another way of estimating Φ would be to assume that electrons come from the bottom of silicon conduction band at the Si/ZrO_2 interface. This is particularly relevant for thin oxide films where electrons can tunnel from the interface into defect states [18]. Theoretical estimates [19] of the valence band offset (3.3 eV) at the interface and the band gap of Si (1.1 eV) are shown in Fig. 4.

Table 1
Ionization potential $I_p(D)$, electron $\chi_e(D)$ and hole $\chi_h(D)$ affinities (in eV) of defects in different charge states

D	V_4^0	V_4^+	V_4^{2+}	O_3^0	O_3^-	O_3^{2-}
$I_p(D)$	4.23	4.41	–	5.82	5.62	5.62
$\chi_e(D)$	–	3.76	3.97	4.16	5.05	–
$\chi_h(D)$	2.07	1.86	–	0.07	1.67	0.78

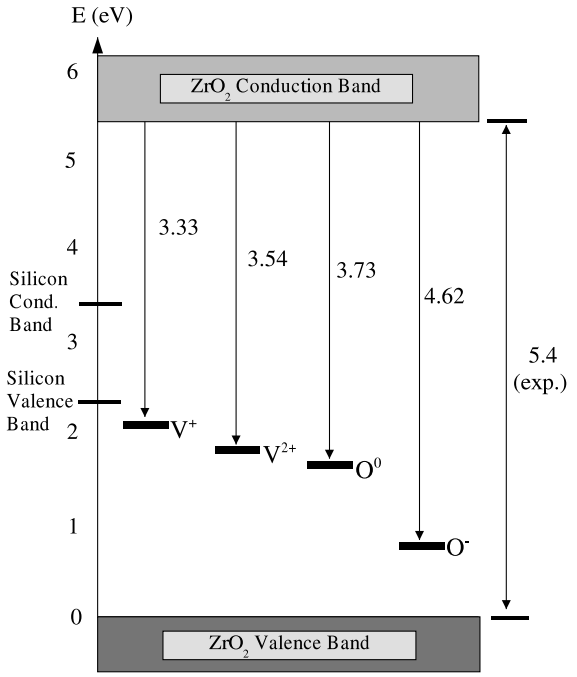

Fig. 4. Energy level diagram showing the electron affinities for various defects in monoclinic zirconia. All energies are in eV.

We can see that singly and doubly charged vacancies, and neutral and singly charged oxygen interstitials have positive electron affinities for electrons coming from the bottom of the conduction band. The electron affinity for the neutral vacancy cannot be accurately predicted because the electron state is lying at the bottom of the conduction band and depends on the accuracy of calculation of the conduction band. From Fig. 4, we can also see that doubly and singly charged vacancies, and neutral and single-charged oxygen interstitials can serve as traps for electrons at the bottom of the silicon conduction band.

5. Conclusions

The results of the calculations demonstrate that oxygen interstitials and vacancies are strongly localised. They produce electronic states in the band gap, and O_3^0 and O_3^-, V_4^{2+}, and V_4^+ centres can serve as electron traps. They have similar formation energies and properties to analogous defects in other cubic oxides, silica and alkali halides.

These results also allow us to estimate the formation energy of a neutral vacancy-oxygen atom Frenkel defect pair, which is about 7.3 eV (with respect to the oxygen atom in the triplet state). This compares well with empirical calculations which found an energy of 9.1 eV [20] for the anion Frenkel pair and also with ab initio calculations of zircon [8] which also found an energy of 7.3 eV. This energy is much larger than the band gap, suggesting that recombination of electron–hole pairs created by crystal excitation with electrons or photons cannot create Frenkel defect pairs as it does in alkali halides or silica. This is in agreement with the well-known radiation stability of zirconia.

Acknowledgements

The authors wish to thank M. Szymanski, M. Hakala and A.M. Stoneham for useful discussions. ASF wishes to thank the Centre for Scientific Computing, Helsinki for use of its computational resources. We are grateful to EPSRC and Fujitsu for financial support of this work. The *lev*00 code [21] was used for calculation of density maps and DOS.

References

[1] T.S. Jeon, J.M. White, D.L. Kwong, Appl. Phys. Lett. 78 (2001) 368.
[2] M. Copel, M. Gribelyuk, E. Gusev, Appl. Phys. Lett. 76 (2000) 436.
[3] A.S. Foster, V.B. Sulimov, F. Lopez-Gejo, A.L. Shluger, R.M. Nieminen, Phys. Rev. B 64 (2001) 224108.
[4] G. Kresse, J. Furthmüller, Comput. Mater. Sci. 6 (1996) 15.
[5] G. Kresse, J. Furthmüller, Phys. Rev. B 54 (1996) 11169.
[6] D. Vanderbilt, Phys. Rev. B 41 (1990) 7892.
[7] G. Kresse, J. Hafner, J. Phys.: Condens. Matter 6 (1994) 8245.
[8] J.P. Crocombette, Phys. Chem. Miner. 27 (1999) 138.
[9] D.R. Hamann, Phys. Rev. Lett. 81 (1998) 3447.
[10] G. Pacchioni, G. Ieranò, Phys. Rev. B 56 (1997) 7304.
[11] M.A. Szymanski, A.M. Stoneham, A.L. Shluger, Microelectron. Reliab. 40 (2000) 567.
[12] E. Scorza, U. Birkenheuer, C. Pisani, J. Chem. Phys. 107 (1997) 9645.
[13] V. Sulimov, S. Casassa, C. Pisani, J. Garapon, B. Poumellec, Modell. Simul. Mater. Sci. Eng. 8 (2000) 763.

[14] D. Nagle, V.R. Paiverneker, A.N. Petelin, G. Groff, Mater. Res. Bull. 24 (1989) 619.
[15] R.H. French, S.J. Glass, F.S. Ohuchi, Y.N. Xu, W. Ching, Phys. Rev. B 49 (1994) 5133.
[16] D.W. McComb, Phys. Rev. B 54 (1996) 7094.
[17] B. Králik, E.K. Chang, S.G. Louie, Phys. Rev. B 57 (1998) 7027.
[18] W.B. Fowler, J.K. Rudra, M.E. Zvanut, F.J. Feigl, Phys. Rev. B 41 (1990) 8313.
[19] J. Robertson, J. Vac. Sci. Technol. B 18 (2000) 1785.
[20] W.C. Mackrodt, P.M. Woodrow, J. Am. Ceram. Soc. 69 (1986) 277.
[21] L.N. Kantorovich, 1996–2001, unpublished. Available from <www.cmmp.ucl.ac.uk/~lev/codes/lev00/index.html>.